Equation of state of the one-component plasma derived from precision Monte Carlo calculations

Guy S. Stringfellow*
Lick Observatory, Board of Studies in Astronomy and Astrophysics, University of California, Santa Cruz, California 95064
and Institute of Geophysics and Planetary Physics, Lawrence Livermore National Laboratory, Livermore, California 94550

Hugh E. DeWitt†
Institute for Nonlinear Sciences, University of California, Santa Cruz, California 95064

W. L. Slattery
Los Alamos National Laboratory, Los Alamos, New Mexico 87545
(Received 9 June 1989; revised manuscript received 5 September 1989)

Analytical fits to the one-component plasma (OCP) equation of state have been derived for internal energies that have reduced all N-dependent effects to within the statistical uncertainties introduced by the Monte Carlo computational process, which themselves are very small. Values of $N \gtrsim 500$ adequately represent the thermodynamic limit. Using the fluid internal energies for only $N=686$, various analytical fits are generated, compared, and discussed. The thermal energy is accurately represented by a simple power-series fit with the leading term given by $\Gamma^{1/3}$, but also requires a small correction to the bcc Madelung term that brings that coefficient down to nearly -0.9, the value derived for hypernetted-chain theory. The fluid thermal energy data are reproduced to better than 0.2% over all Γ by our fit(s). The solid phase requires *both* anharmonic terms to be included in the fit, implying that the previous justification for dropping the first anharmonic correction is unwarranted. The location of the fluid-solid phase transition utilizing these new fits yields $\Gamma_{\rm bcc}=178$ and $\Gamma_{\rm fcc}=192$.

Monte Carlo simulations of the classical one-component plasma (OCP) have been used extensively during the past two decades to obtain the OCP fluid equation of state (EOS) and the location of the fluid-solid phase transition.[1-7] The use of the Monte Carlo results is made difficult by the fact that the thermal energy ($U_{\rm th}/NkT$) is less than 2% of the total energy (U/NkT) at high Γ near the phase transition. Reliable results require that $U_{\rm th}/NkT$ be known to an accuracy of about a tenth of a percent in both phases. The Monte Carlo results are very sensitive to any number dependence for the ions (N dependence) that may exist in the numerical simulations. Using data calculated for a wide variety of N, Slattery, Doolen, and DeWitt[5] (SDD[5]) made an attempt to account for the behavior of the N dependence by adding a term to their fit for the EOS of the form $e\Gamma/N$, where e is a constant generated by the fit and used for obtaining results in the limit $N\rightarrow\infty$.

Rather than trying to use the data for different values of N, as in these previous studies, in this paper we obtain very accurate fluid internal energy and Helmholtz free-energy expressions utilizing only data for $N=686$. We have found this to be a sufficiently large enough N for the fluid phase such that any residual number dependence is less than or equivalent to the unavoidable statistical error inherent in the Monte Carlo simulations. Consider the radial pair distribution functions $g(r)$ for $N=500$ and 686, which are displayed in Fig. 1 for two values of Γ, one on each side of the phase transition. For each Γ the fluid curves for $N=500$ and 686 have essentially identical radial distribution functions out to at least seven ion sphere radii, which is the reason for the internal energies being statistically equivalent (see also Table I). Therefore, $N\geq 500$ accurately reflects the thermodynamic limit. Note that, at these values of N, the center-of-mass correction proposed by Hoover *et al.*[8] is negligible, falling within the statistical errors of our data. In the solid phase, however, the plasma can freeze into either a face-centered-cubic (fcc; $N=4n^3$ where n is an integer ≥ 1) or body-centered-cubic (bcc; $N=2n^3$) configuration, depending on the value of N. Thus there is an energy difference between the bcc and fcc high-N solid data due to the lattice structure of the two configurations (see Fig. 1). Utilizing these results, we will now proceed to obtain the equation of state for the OCP in both the fluid and solid phase. We use only the $N=686$ data of SDD[5], supplemented (or replaced) by the values presented here for the fluid phase, thereby avoiding the introduction of additional systematic errors. Our new values of the Monte Carlo internal energies $U_{\rm MC}$ are given in Table I.

DeWitt[3] originally studied fits to the OCP internal energy fluid data[1] of the form

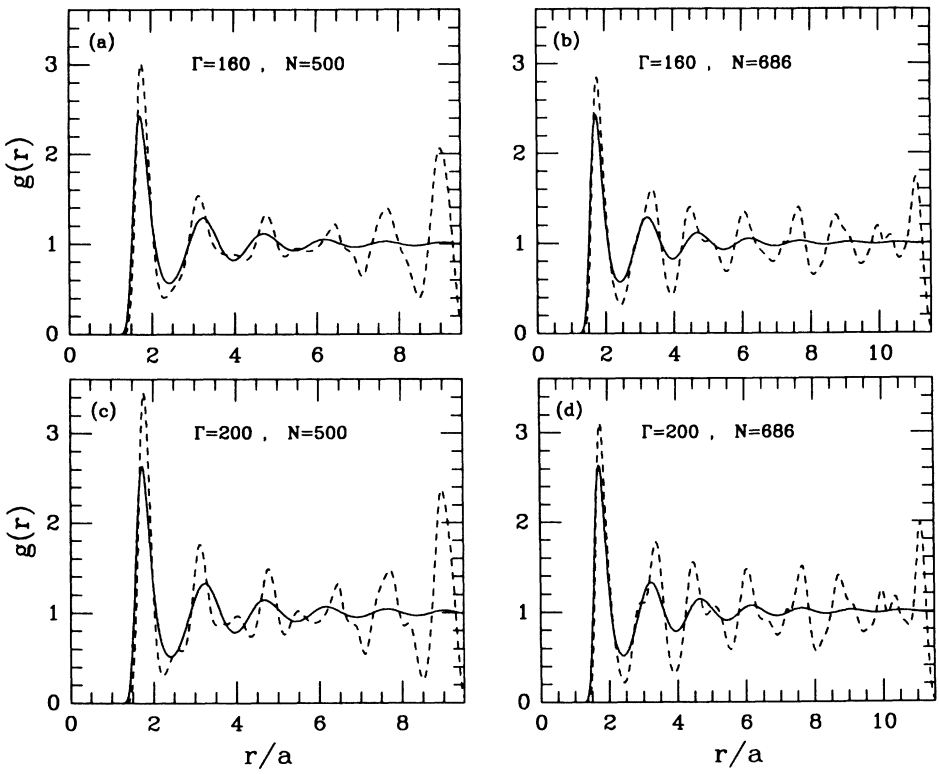

FIG. 1. Comparison of the bcc and fcc particle pair correlation functions $g(r)$ for high N plotted against the ion separation r (in units of the ion sphere radius) at several Γ in the fluid and solid phase: (a) at $\Gamma=160$ the fluid (solid curve) and solid (dashed line) phases are presented for $N=500$; (b) the same as (a) except for $N=686$; (c) $\Gamma=200$ for $N=500$; and (d) the same as (c) but for $N=686$.

$$\frac{U_{\mathrm{MC}}}{NkT}=a\Gamma+b\Gamma^{s}+c \tag{1}$$

from which he concluded that $s=0.25\pm0.02$ for $\Gamma\leq 40$ and $s=0.3\pm0.1$ for $\Gamma\geq 50$. The high-Γ data, back then, was simply not accurate enough to allow a precise fit over the entire range of Γ. In addition, the coefficient a differed markedly from the Madelung bcc lattice value when left as a free parameter in the fit to be determined by the data. Subsequently, DeWitt and Rosenfeld[9] applied a variational hard-sphere calculation that included the virial entropy and found that the form of the internal energy could be expressed as

TABLE I. New Monte Carlo internal energies, uncorrected for center-of-mass motion, computed for selected values of N. Initial conditions (IC) are either fluid (F) or lattice (L).

Γ	$\frac{U_{\mathrm{MC}}}{NkT}$	$\pm\sigma$	N	Thermalizations ($\times10^6$)	Configurations ($\times10^6$)	IC
			bcc			
150	−132.1070	0.0016	686	0.1	31.9	F
160	−141.7254	0.0010	686	2.0	77.2	L
180	−158.8972	0.0008	686	1.0	143.0	F
180	−159.6684	0.0009	686	32.0	80.0	L
200	−176.7739	0.0011	686	11.0	83.0	F
200	−177.6060	0.0010	686	0.7	46.5	L
			fcc			
160	−141.0381	0.0012	500	2.0	78.0	F
160	−141.7006	0.0010	500	0.5	111.5	L
180	−158.8943	0.0012	500	6.0	90.0	F
180	−159.6489	0.0010	500	0.1	79.9	L
200	−176.7697	0.0010	500	2.0	142.0	F
200	−177.5856	0.0010	500	0.1	79.9	L

$$\frac{U_{\rm MC}}{NkT}=a\Gamma+b\Gamma^{1/4}+c+d\Gamma^{-1/4}\ , \tag{2}$$

in agreement with the form of the fit [Eq. (1)] found previously.[3] Since then, Eq. (2) has been used to represent the EOS for the OCP.[4-7]

Since we are interested in discovering the best empirical representation of the EOS, we have chosen to generalize Eq. (2) to the form found in Eq. (1) and to explore a broad range in the parameter s. Since it does not matter whether the internal energy or thermal energy is chosen to be fit, we elect to use the latter. Hence we will be dealing with a fit function of the generalized form

$$\frac{U_{\rm th}}{NkT}=\delta a\Gamma+b\Gamma^{s}+c+d\Gamma^{-s}\ , \tag{3}$$

where $U_{\rm th}=(U_{\rm MC}-U_{\rm bcc})$. Here δa represents the amount by which the term $a\Gamma$ differs from the bcc Madelung term where $a_{\rm bcc}=-0.895\,929$,

$$a\Gamma=(a_{\rm bcc}+\delta a)\Gamma\ . \tag{4}$$

Notice that we have constrained the terms with coefficients b and d in Eq. (3) to have the same value of the exponent s. In so doing we preserve the ability to express our final fit in terms of a single power-series expansion in s. Thus we have four independent parameters (δa, b, c, and d) in which a linear least-squares fitting[9] can be performed for various values of s.

We explore a range of $0.20\le s\le 0.50$. A sample of these fits are presented in Table II, which lists the coefficients and the resulting standard deviation σ (the square root of Eq. 14.1.5 in Ref. 10) for each fit. The internal energies and their associated errors have been rounded off to three decimal places when fitting. Previous fits[3-5,8] to the OCP have not taken into account the experimental (numerical) errors as we do here. The first striking observation, which is obvious from these results, is that an accurate fit to the data requires $\delta a\neq 0$. Coupled with this is the surprising result that the coefficient a is *very close* to, but slightly larger than, -0.9; the exact value recently derived for the coefficient of the Madelung term in the hypernetted-chain approximation (HNC).[11] However, the HNC equations yield power-series expansions in s of $\frac{1}{2}$ (i.e., $-0.9\Gamma+b\Gamma^{1/2}+\cdots$). This is the

TABLE II. Linear least-squares fits to the $N=686$ (bcc) data in Table I and SDD[5]. Each functional form is given prior to listing the coefficients resulting from the fit. The parameter s is the exponent of Γ in the function, and δa is the difference required by the fitting process over that of $a_{\rm bcc}$, the bcc value of the Madelung constant. The standard deviation, which we use as a quantitative measure of how "good" the fits are, is denoted here as σ. The absence of an entry implies that term was not used in the fitting function. Powers of 10 are given in square brackets.

s	δa	a	b	c	d	$10^2\sigma$
			$U_{\rm th}/NkT=b\Gamma^{s}+c$			
0.20		−0.895 929	1.110 153	−0.802 975		4.80
0.25		−0.895 929	0.795 416	−0.471 288		4.14
0.30		−0.895 929	0.586 695	−0.244 360		8.50
1/3		−0.895 929	0.483 579	−0.128 644		11.50
0.35		−0.895 929	0.439 884	−0.078 566		12.92
0.50		−0.895 929	0.192 813	−0.022 505		22.49
			$(U_{\rm MC}+0.9\Gamma)/NkT=b\Gamma^{s}+c$			
0.25	−4.071 00 [−3]	−0.900 000	0.960 506	−0.669 656		12.88
0.30	−4.071 00 [−3]	−0.900 000	0.713 343	−0.402 447		5.74
1/3	−4.071 00 [−3]	−0.900 000	0.590 673	−0.265 690		1.54
0.35	−4.071 00 [−3]	−0.900 000	0.538 536	−0.206 357		1.05
0.50	−4.071 00 [−3]	−0.900 000	0.240 904	0.156 539		14.85
			$U_{\rm th}/NkT=\delta a\Gamma+b\Gamma^{s}+c$			
0.25	−6.727 90 [−4]	−0.896 602	0.822 700	−0.504 071		2.55
0.30	−2.362 81 [−3]	−0.898 292	0.660 202	−0.336 114		0.81
1/3	−3.648 30 [−3]	−0.899 577	0.579 554	−0.251 460		0.43
0.35	−4.345 51 [−3]	−0.900 275	0.545 188	−0.214 974		1.01
0.40	−6.688 68 [−3]	−0.902 618	0.460 076	−0.123 001		2.80
0.50	−1.285 71 [−2]	−0.908 786	0.344 697	0.008 672		6.38
			$U_{\rm th}/NkT=\delta a\Gamma+b\Gamma^{s}+c+d\Gamma^{-s}$			
0.25	−2.102 11 [−3]	−0.898 031	0.969 821	−0.866 074	0.222 700	0.40
0.30	−2.845 06 [−3]	−0.898 774	0.692 060	−0.417 913	0.052 585	0.21
1/3	−3.446 15 [−3]	−0.899 375	0.569 333	−0.224 470	−0.017 875	0.19
0.35	−3.782 27 [−3]	−0.899 711	0.520 112	−0.147 826	−0.045 145	0.24
0.40	−4.952 48 [−3]	−0.900 881	0.406 187	0.027 318	−0.105 785	0.52
0.50	−8.231 58 [−3]	−0.904 161	0.270 085	0.232 832	−0.173 256	1.24

reason for extending the range of the exponent s to $\frac{1}{2}$ in the fits presented here.

We can see from Table II that the fits with $s=\frac{1}{2}$ are not good at all. Hence the HNC theory derived for the second-order terms (beyond the Madelung term) are not appropriate for the fluid Monte Carlo results. Instead, we are zeroing in on a value of $s\approx\frac{1}{3}$. This value of s is quite different from those previously determined.[1-7,9] A small variation about this value, $s\sim 0.30$–0.35, also gives pretty good fits to the fluid data as long as three or more terms are included, but only with $\delta a\neq 0$. Let us closely examine some of our best statistical fits taken from Table II for the various functional forms listed there. These fits are graphically presented in Fig. 2, where in the main portion of the figure the thermal energy is plotted for the entire range of Γ while the insert shows an enlarged view for the region from $80\leq\Gamma\leq 200$. The actual $N=686$ fluid data are given by the open squares. In the insert the vertical height of the square corresponds to $\Delta U_{\rm th}/NkT=0.006$, equivalent to an error of ± 0.003. Thus, if a fit that reproduces the fluid thermal energy data to $\lesssim 0.15\%$ is desired (as discussed above), then the curves in Fig. 2 should at least pass through the sides of every square in the insert at each Γ.

The series of fits with two terms and the constraint $\delta a=0$ are clearly unacceptable, and if extended to include a third term ($d\Gamma^{-s}$), the fits are even worse. This implies that the first term in the analytical fit cannot be the Madelung term for a bcc lattice. All of the two-term fits with $a=-0.9$ are also not accurate enough and deviate noticeably from the real data; as seen in Fig. 2, the best fit using this form overestimates the thermal energy of the system for $\Gamma>60$. The best three-term fit with $a=-0.9$ (see dotted curve in Fig. 2) is fairly good everywhere over the region $110\leq\Gamma\leq 180$, but the thermal energies are overestimated for $\Gamma<110$ and underestimated for $\Gamma\gtrsim 180$. The fit is noticeably bad close to the phase transition. Our most accurate fits are for $s=\frac{1}{3}$ with three or four terms where the coefficient a remains completely unconstrained. These are shown in Fig. 2 as the dashed and solid curves, respectively. The four-term fit is the most accurate over the entire range in Γ, behaving well near the phase transition *and below* $\Gamma=110$. This latter point is crucial in accurately determining the location of the phase transition since the free energies are an integral property of the internal energies. While the addition of the extra term $d\Gamma^{-s}$ fine tunes an already very good fit, the three-term fit simplifies the resulting expression for the equation of state, but at the expense of some accuracy.

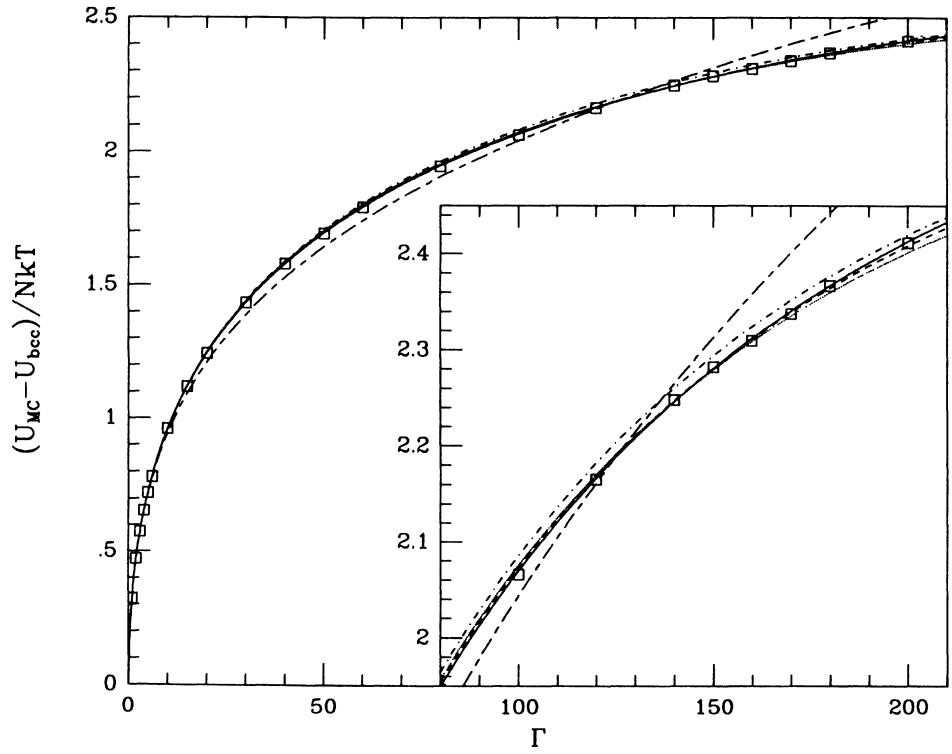

FIG. 2. Analytical fits to the fluid thermal energy $N=686$ data (open squares; SDD[5], and Table I) of the form given by Eq. (3) are plotted for the entire Γ range in the main portion of the figure. The inset shows an expanded view of $U_{\rm th}/NkT$ for $80\leq\Gamma\leq 210$. Shown are the fits for $\delta a=d=0$ with $s=0.25$ (long-short dashed curve); $a=-0.9$, $d=0$ with $s=0.35$ (dot-dashed curve); $a=-0.9$ and $s=0.35$ (dotted curve); $s=\frac{1}{3}$, $d=0$ (dashed curve); and $s=\frac{1}{3}$ (solid curve), with a unconstrained for these latter two, our *best fits*. Except for the dotted curve ($a=-0.9$, $b=0.531\,685$, $c=-0.176\,699$, $d=-0.027\,067$, $\sigma=0.0061$), see Table II for the appropriate values of the coefficients. In the inset the vertical extent of the open squares have $\Delta U_{\rm th}/NkT=0.006$, which is equivalent to an error of ± 0.003 and $\lesssim 0.15\%$ of $U_{\rm th}/NkT$ at large Γ.

Of course, one imagines that the more terms that are added to the fit, the "better" one can potentially reproduce the data. However, it has been our experience that this is true only for judicious choices of the terms being added. Bad choices require even further terms being added to rectify their harm; for example, the two- and three-term fits with $a = a_{\rm bcc}$. Extra terms complicate unnecessarily the deduced form of the equation of state. A simple three- or four-term fit is much more desirable than other tedious functional forms in application. The fits produced herein strongly indicate that a power series expansion of the form Γ^s with $s \approx \frac{1}{3}$ and a very close to, but just slightly larger than, -0.9 is appropriate. Currently, there are limited theories that generate series expansions with $s = \frac{1}{2}$ (which also yields the -0.9 coefficient exactly[11]) and $s = \frac{1}{4}$,[9] but nothing yet that produces $s = \frac{1}{3}$. Further work is required to incorporate a theory than can explain our new results.

The thermal energy in the solid phase has been successfully reproduced using the functional form[2]

$$\frac{U_{\rm th}}{NkT} = 1.5 + f\Gamma^{-1} + h\Gamma^{-2} . \tag{5}$$

The first term in Eq. (5) comes from harmonic theory and the last two terms are anharmonic corrections derived from perturbation theory whose contributions provide minor but important adjustments to the thermal energy, in particular at lower values of Γ near the phase transition. In Fig. 3 the solid data for $N = 500$ and 686 clearly show the sizeable difference between the fcc and bcc configurational energies, so we must fit each set of data to Eq. (5). Our new fits to the $N = 500$ and 686 data in Fig. 3 are indicated by the dot-dashed and solid curves, respectively. For comparison, we show the fit of Ref. 6 (dotted curve) to the fcc $N = 108$ data[4] (inverted triangles) and our fit to the bcc $N = 686$ data without the $f\Gamma^{-1}$ term in Eq. (5) (dashed curve). Also shown are the bcc $N = 128$ $U_{\rm MC}$ data[5] (triangles).

Table III gives the fitted coefficients f and h in Eq. (5) to the fcc and bcc data in the solid phase. Our fit to the bcc $N = 686$ data *with both anharmonic terms* accurately reproduces even the highest-Γ thermal energies (i.e., $\Gamma = 300$). This is not the case with the old SDD[5] fit that included only the $h\Gamma^{-2}$ term in Eq. (5). Pollack and Hansen[2] showed in their appendix that the coefficient of Γ^{-1} is zero in a cell model calculation for the OCP, but this is not a rigorous proof. If the thermal energy data below $\Gamma < 240$ is to be fitted simultaneously with that for $\Gamma \geq 240$ to within the desired accuracy, then the first term must be nonzero, as a comparison of our fits in Fig. 3 shows. Note that if we force the Γ^{-1} term in Eq. (5) to vanish, we essentially reproduce the fit obtained by SDD[5]. Our new fcc $N = 500$ solid data have lower thermal energies and are statistically more accurate than the $N = 108$ data previously used, and for these reasons is

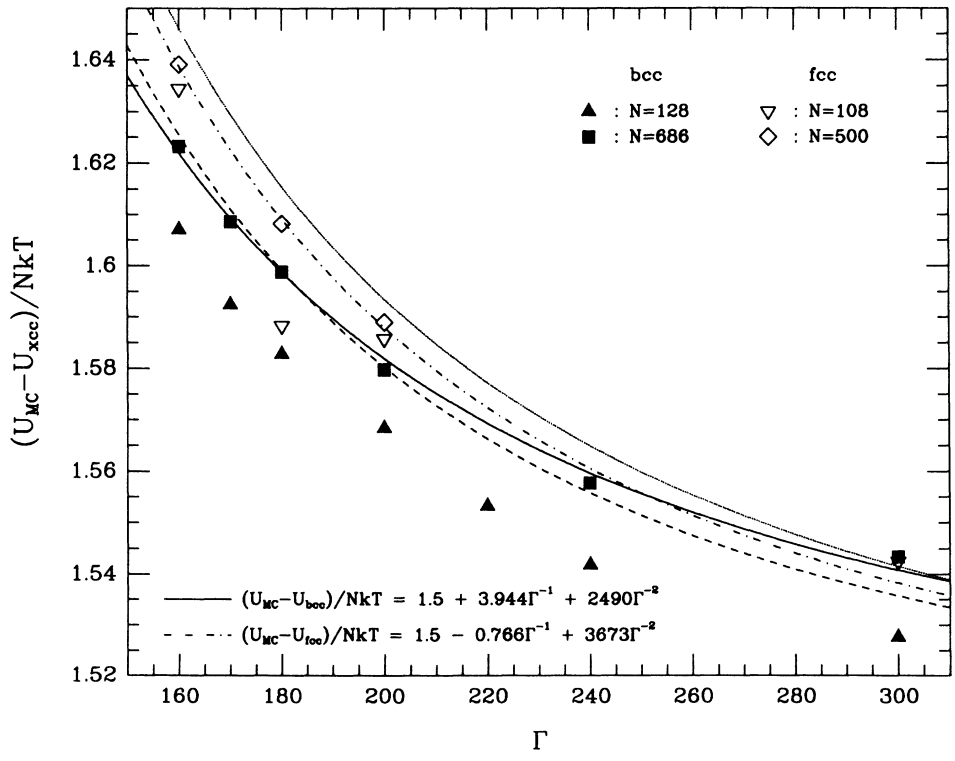

FIG. 3. Thermal energy in the solid phase for both the bcc and fcc data. Here we represent the generic Madelung term as $U_{\rm xcc}$ since the thermal energy is defined as the excess energy over the respective lattice configuration. The various analytical fits shown are our fit to Eq. (5) for the $N = 686$ data (solid curve), and excluding the $f\Gamma^{-1}$ term (dashed curve); our fit to the fcc $N = 500$ data with or without the first anharmonic term (dotted curve); the fit of Ref. 6 to the $N = 108$ data of Ref. 4 (dot-dashed curve).

TABLE III. Linear least-squares fit of the form given by Eq. (5) to the bcc $N=686$ and fcc $N=500$ solid data (uncorrected for the center-of-mass motion) from SDD[5] and this paper (Table I).

f	h	$10^3\sigma$
	bcc $N=686$	
	3212	3.63
3.9437	2490	1.73
	fcc $N=500$	
	3544	0.79
−0.7660	3673	0.70

preferred over the fit obtained by Ref. 6. The fact that we have only three thermal energy values makes it irrelevant whether one or two anharmonic terms are included in the fit to $N=500$; both of the fits presented in Table III in this case differ almost imperceptibly from one another. We must emphasize strongly that none of the curves are guaranteed to be valid, yet alone accurate, if extrapolated beyond the range of the data being fit. This is exemplified by the crossing of the fits to the $N=500$ and 686 solid thermal energies in Fig. 3. This is physically inconsistent; the fcc lattice will always have thermal energies higher than or, in the limit as $\Gamma\to\infty$, equal to those for the $N=686$ lattice. We expect the fcc lattice ($N=500$) thermal energies to behave similar to those of the bcc lattice ($N=686$) at high Γ.

The location of the fluid-solid phase transition is determined by finding the Γ where the free energies of the fluid and solid are equal. For Γ's above this critical value the solid is more stable than the fluid, having lower thermal energies. Equation (3) yields a general Helmholtz fluid free-energy expression

$$\frac{F}{NkT}=a\Gamma+\frac{b}{s}\Gamma^{s}-\frac{d}{s}\Gamma^{-s}+(3+c)\ln\Gamma-\left[a+\frac{b-d}{s}+1.1516\right]. \tag{6}$$

The integral from $0\le\Gamma\le 1$ evaluated by SDD[5], including the ideal gas contribution,[1] leads to the value -1.1516 in Eq. (6). The free energy in the solid phase is given by the sum of harmonic and anharmonic contributions. The harmonic contribution is taken from Ref. 2 [Eq. (2.10)] and the anharmonic contribution to the internal energy in Eq. (5) is integrated over Γ from ∞ down to some finite value. Putting all this together yields

$$\frac{F}{NkT}=\begin{Bmatrix}\frac{U_{\rm bcc}}{NkT}\\ \frac{U_{\rm fcc}}{NkT}\end{Bmatrix}+\frac{9}{2}\ln\Gamma-f\Gamma^{-1}-\frac{h}{2}\Gamma^{-2}-\begin{Bmatrix}1.8856, & \text{for bcc}\\ 1.8454, & \text{for fcc}\end{Bmatrix} \tag{7}$$

for the bcc and fcc lattice configurations. The entropy constants in Eq. (7) result from the sum over the normal mode vibrations of the ions in the crystal in the limit $N\to\infty$ and have been provided by Folland.[12] The bcc entropy constant agrees to four decimal places with the value used in other studies,[2] but the value for the fcc lattice in Eq. (7) is smaller by 0.0110 than that computed by Helfer, McCrory, and Van Horn.[6] Both the bcc and fcc lattice thermal energies approach 1.5 in the limit $\Gamma\to\infty$. Let us now discuss the location of the phase transition, first in terms of a transition to the bcc lattice, for specific cases of the fluid and solid free energies. Consider our best overall fit: Eq. (3) with $s=\frac{1}{3}$ and $a\neq a_{\rm bcc}$ or -0.9. We find that $\Gamma_{\rm bcc}=180.5$ with $f=0$ for the solid free energy in Eq. (7), and $\Gamma_{\rm bcc}=178.0$ if *both* anharmonic terms are included. The former value agrees with Ref. 7, which used a fit derived from various values of N to different groups fluid data, and the latter value is exactly that found by SDD[5]; both used the SDD[5] fit to the solid that neglected the first anharmonic term $f\Gamma^{-1}$.

Generally speaking, the phase transition from the fluid to the fcc lattice always occurs at a value larger than $\Gamma_{\rm bcc}$ for our fits. Specifically, $\Gamma_{\rm fcc}=13.5+\Gamma_{\rm bcc}$, where $\Gamma_{\rm bcc}$ corresponds to the critical Γ using the bcc solid fit with both anharmonic terms included. This gives $\Gamma_{\rm fcc}=192$ for our "best fluid fit" (four-term fit with $s=\frac{1}{3}$ and a unconstrained). Comparing the fluid free energy for this fit with the free-energy expression presented by Helfer, McCrory, and Van Horn,[6] but with our value of the entropy constant, we get $\Gamma_{\rm fcc}=193.5$, whereas they obtained $\Gamma_{\rm fcc}=196$. The free-energy curves for the fluid and solid lie *very close* to one another over a small range in Γ whether the transition occurs to the bcc or fcc lattice. It seems plausible that perturbations to the system occurring near the phase transition could alter the exact values for either $\Gamma_{\rm bcc}$ or $\Gamma_{\rm fcc}$. There is probably an intrinsic uncertainty of about ± 2 in the critical Γ because of this and other uncertainties introduced through the fluid and solid fits.

We would like to thank Nathan Folland, Dieter Hartmann, Anthony Haymet, Karl Kratky, and Yaacov Rosenfeld for useful discussions and/or correspondence. One of us (G.S.S.) acknowledges support from the National Science Foundation Grant No. AST-8521636, and the Institute of Geophysics and Planetary Physics at the Lawrence Livermore National Laboratory. Part of this work has been conducted under the auspices of a special NASA Astrophysics Theory Program (G.S.S.) that supports a joint Center for Star Formation Studies at the NASA-Ames Research Center, the University of California at Berkeley, and the University of California at Santa Cruz, and of the U.S. Department of Energy by the Lawrence Livermore National Laboratory (H.E.D. and G.S.S.) under Contract No. W-7405-ENG-48.

*Present address: Mount Stromlo and Siding Spring Observatories, Institute of Advanced Study, Australian National University, Canberra, Australian Capital Territory 2601, Australia.

†Permanent address: Lawrence Livermore National Laboratory, Livermore, California 94550.

[1]J. P. Hansen, Phys. Rev. A **8**, 3096 (1973).

[2]E. L. Pollock and J. P. Hansen, Phys. Rev. A **8**, 3110 (1973).

[3]H. E. DeWitt, Phys. Rev. A **14**, 1290 (1976).

[4]W. L. Slattery, G. D. Doolen, and H. E. DeWitt, Phys. Rev. A **21**, 2087 (1980).

[5]W. L. Slattery, G. D. Doolen, and H. E. DeWitt, Phys. Rev. A **26**, 2255 (1982), indicated by (SDD[5]) in the text.

[6]H. L. Helfer, R. L. McCrory, and H. M. Van Horn, J. Stat. Phys. **37**, 577 (1984).

[7]S. Ogata and S. Ichimaru, Phys. Rev. A **36**, 5451 (1987).

[8]W. G. Hoover, M. Ross, K. W. Johnson, D. Henderson, J. A. Barker, and B. C. Brown, J. Chem. Phys. **52**, 4931 (1970).

[9]H. E. DeWitt and Y. Rosenfeld, Phys. Lett. **75A**, 79 (1979).

[10]W. H. Press, B. P. Flannery, S. A. Teukolsky, and W. T. Vetterling, *Numerical Recipes* (Cambridge University Press, Cambridge, 1986).

[11]Y. Rosenfeld, Phys. Rev. A **33**, 2025 (1986).

[12]N. O. Folland (private communication).